



# Pazopanib attenuated bleomycin-induced pulmonary fibrosis via suppressing TGF- $\beta$ 1 signaling pathway

Kai Huang<sup>1#</sup>, Qianyi Zhang<sup>1#</sup>, Hao Ruan<sup>2#</sup>, Chunyu Guo<sup>2</sup>, Shuyang Wu<sup>1</sup>, Qinyi Liu<sup>1</sup>, Deqiang Zhang<sup>1</sup>, Shida Long<sup>1</sup>, Wenrui Wang<sup>1</sup>, Zhou Wu<sup>2</sup>, Li Tian<sup>2</sup>, Shuangyan Gao<sup>2</sup>, Huanan Zhao<sup>2</sup>, Xiaoting Gu<sup>1</sup>, Huijun Yin<sup>2</sup>, Cheng Yang<sup>1</sup>

<sup>1</sup>State Key Laboratory of Medicinal Chemical Biology, College of Pharmacy and Tianjin Key Laboratory of Molecular Drug Research, Nankai University, Tianjin, China; <sup>2</sup>China Resources Biopharmaceutical Co., Ltd., Beijing, China

**Contributions:** (I) Conception and design: K Huang, Q Zhang, H Ruan, S Wu, Q Liu, D Zhang; (II) Administrative support: C Yang; (III) Provision of study materials or patients: K Huang, X Gu, C Yang; (IV) Collection and assembly of data: K Huang, Q Zhang, H Ruan, S Long, W Wang, Z Wu, Li Tian, S Gao, H Zhao; (V) Data analysis and interpretation: All authors; (VI) Manuscript writing: All authors; (VII) Final approval of manuscript: All authors.

<sup>#</sup>These authors contributed equally to this work.

**Correspondence to:** Cheng Yang, PhD. State Key Laboratory of Medicinal Chemical Biology, College of Pharmacy and Tianjin Key Laboratory of Molecular Drug Research, Nankai University, Haihe Education Park, 38 Tongyan Road, Tianjin 300353, China. Email: cheng.yang@nankai.edu.cn; Huijun Yin, PhD. China Resources Biopharmaceutical Co., Ltd., No. 2 North Third Ring Middle Road, Anzhen Street, Chaoyang District, Beijing 100000, China. Email: huijunyin@yeah.net; Xiaoting Gu, PhD. State Key Laboratory of Medicinal Chemical Biology, College of Pharmacy and Tianjin Key Laboratory of Molecular Drug Research, Nankai University, Haihe Education Park, 38 Tongyan Road, Tianjin 300353, China. Email: guxiaoting320@126.com.

**Background:** Idiopathic pulmonary fibrosis (IPF) is a chronic and progressive interstitial lung disease with a high mortality rate and limited treatment efficacy. Nintedanib, a tyrosine kinase inhibitor, is clinically used to treat pulmonary fibrosis. At present, only nintedanib is on the market for the treatment of pulmonary fibrosis. Pazopanib is a drug for the treatment of renal cell carcinoma and advanced soft tissue sarcoma.

**Methods:** In this study, we explored whether pazopanib can attenuate bleomycin (BLM)-induced pulmonary fibrosis and explored its antifibrotic mechanism. *In vivo* and *in vitro* investigations were carried out to investigate the efficacy and mechanism of action of pazopanib in pulmonary fibrosis.

**Results:** *In vivo* experiments showed that pazopanib can alleviate pulmonary fibrosis caused by BLM, reduce the degree of collagen deposition and improve lung function. *In vitro* experiments showed that pazopanib suppressed transforming growth factor- $\beta$ 1 (TGF- $\beta$ 1)-induced myofibroblast activation and promoted apoptosis and autophagy in myofibroblasts. Further mechanistic studies demonstrated that pazopanib inhibited the TGF- $\beta$ 1/Smad and non-Smad signaling pathways during fibroblast activation.

**Conclusions:** In conclusion, pazopanib attenuated BLM-induced pulmonary fibrosis by suppressing the TGF- $\beta$ 1 signaling pathway. Pazopanib inhibits myofibroblast activation, migration, autophagy, apoptosis, and extracellular matrix (ECM) buildup by downregulating the TGF- $\beta$ 1/Smad signal route and the TGF- $\beta$ 1/non-Smad signal pathway. It has the same target as nintedanib and is a tyrosine kinase inhibitor.

**Keywords:** Pazopanib; pulmonary fibrosis; fibroblast; transforming growth factor- $\beta$ 1 (TGF- $\beta$ 1)

Submitted Aug 28, 2023. Accepted for publication Feb 05, 2024. Published online Apr 16, 2024.

doi: 10.21037/jtd-23-1349

View this article at: <https://dx.doi.org/10.21037/jtd-23-1349>

## Introduction

Idiopathic fibrosis is a progressive interstitial lung disease, the pathogenesis of which is unknown. The pathogenesis of idiopathic fibrosis is related to age. Idiopathic pulmonary fibrosis (IPF) is characterized by abnormal deposition of extracellular matrix (ECM) in the lung (1-3). Due to the aging of the population and the increasing severity of air pollution, the incidence of IPF is increasing annually (4,5). At present, there are only two drugs available on the market for treating idiopathic fibrosis, but their efficacy is limited (6). The development of new drugs for the treatment of IPF has become a hot topic of research and development.

In recent studies, many researchers have agreed that fibroblast activation, myofibroblast apoptosis and autophagy are vital for fibrotic progression (1,7). Transforming growth factor- $\beta$ 1 (TGF- $\beta$ 1) is a well-known core regulator of the development of pulmonary fibrosis (8) and is extremely upregulated in the lungs of IPF patients (9). High levels of myeloid cell activation, migration and proliferation are likely to occur, and TGF- $\beta$ 1 can induce fibroblasts to transform into non-fibroblasts (10). The phosphorylation of Smad2 and Smad3 is promoted by TGF- $\beta$ 1 and mainly acts on Smad2 and Smad3 pathways downstream of TGF- $\beta$ 1 to regulate fibroblast activation and ECM production (11,12). Autophagy is essential for survival, differentiation,

development, and homeostasis because it can promote lysosomal degradation (13). ECM protein overexpression is a catastrophic component in the etiology of pulmonary fibrosis, and autophagy can downregulate the expression of ECM proteins (14,15). In addition, TGF- $\beta$ 1 strongly suppresses interleukin-1 $\beta$  (IL-1 $\beta$ )-induced apoptosis in myofibroblasts through two mechanisms, namely, inhibiting inducible nitric oxide synthase (iNOS) expression and restricting the decrease in Bcl-2 expression (16). Therefore, suppressing TGF- $\beta$ 1-induced fibroblast activation and ECM production and promoting myofibroblast autophagy and intriguing myofibroblast apoptosis are essential for treatment of fibrosis.

Pazopanib is a multityrosine kinase inhibitor with the same targets as nintedanib and was approved by the Food and Drug Administration (FDA) in June 2010 for treating metastatic renal cell carcinoma (RCC) (17,18). Pazopanib also has a positive impact on solitary fibrous tumor (SFT) by decreasing the size of the tumor in clinical trials (19). In a murine xenograft, pazopanib was found to be a possible agent against synovial sarcoma growth mainly via suppression of the PI3K-Akt pathway (18). Pazopanib can induce autophagic flux by increasing the number of LC3-green fluorescent protein (GFP) vesicles in sarcoma cells, the results of which revealed a reduction in tumor volume (20). Pazopanib can decrease the survival of A549 cells, possibly mainly through the induction of apoptotic cell death (21). However, the efficacy and pharmacological mechanism of pazopanib in pulmonary fibrosis have not been reported. In this study, we explored the antifibrotic effect of pazopanib on bleomycin (BLM)-induced pulmonary fibrosis in mice.

Our study clarified that pazopanib plays a key role in alleviating BLM-induced pulmonary fibrosis by suppressing fibroblast activation and promoting myofibroblast autophagy and apoptosis via the inhibition of TGF- $\beta$ 1/Smad and TGF- $\beta$ 1/non-Smad signaling. This study provides a theoretical and experimental basis for the clinical treatment of pulmonary fibrosis with pazopanib. We present this article in accordance with the ARRIVE reporting checklist (available at <https://jtd.amegroups.com/article/view/10.21037/jtd-23-1349/rc>).

## Methods

### *BLM-induced animal model of pulmonary fibrosis*

Six- to 8-week-old male C57BL/6 mice were purchased from Charles River (Beijing, China). All mice were

### Highlight box

#### Key findings

- Pazopanib attenuated bleomycin (BLM)-induced pulmonary fibrosis by suppressing the transforming growth factor- $\beta$ 1 (TGF- $\beta$ 1) signaling pathway.

#### What is known and what is new?

- Pazopanib is a drug for the treatment of renal cell carcinoma and advanced soft tissue sarcoma.
- *In vivo* experiments showed that pazopanib can alleviate pulmonary fibrosis caused by BLM, reduce the degree of collagen deposition and improve lung function. *In vitro* experiments showed that pazopanib suppressed TGF- $\beta$ 1-induced myofibroblast activation and promoted apoptosis and autophagy in myofibroblasts. Further mechanistic studies demonstrated that pazopanib inhibited the TGF- $\beta$ 1/Smad and non-Smad signaling pathways during fibroblast activation.

#### What is the implication, and what should change now?

- Pazopanib attenuated BLM-induced pulmonary fibrosis by suppressing the TGF- $\beta$ 1 signaling pathway. It has the same target as nintedanib and is a tyrosine kinase inhibitor.

**Table 1** Antibody information

Antibody	Company, item No.
Anti-GAPDH	Affinity, AF7021
$\alpha$ -SMA	Affinity, BF9212
Anti-collagen I	Affinity, AF0134
Anti-Smad2	Affinity, AF6449
Anti-Smad3	Affinity, AF6362
Anti-Akt1/2/3	Affinity, AF6259
Anti-Erk1/2	Affinity, AF0155
Anti-caspase3	Affinity, AF6311
Anti-caspase7	Affinity, AF5118
Anti-caspase9	Affinity, AF6348
Anti-SQSTM1/P62	CST, 5144
Anti- $\beta$ -tubulin	Affinity, AF7011
Anti-fibronectin	Affinity, AF0738
Anti-LC3A/B	CST, 4018
Anti-p-Smad2 (Ser467)	Affinity, AF3449
Anti-p-Smad3 (Ser423 + Ser425)	Affinity, AF8315
Anti-p-Akt1/2/3 (Ser473)	Affinity, AF0016
Anti-p-Erk1/2 (Thr202 + Thr204)	Affinity, AF1015
Anti-cleaved-caspase3 (Asp175, p17)	Affinity, AF7022
Anti-cleaved-caspase7 (Asp198)	Affinity, AF4023
Anti-cleaved-caspase9 (Asp353)	Affinity, AF5240

housed and cared for in a pathogen-free facility at Nankai University Experimental Animal Center. The Nankai University Institutional Animal Care and Use Committee (IACUC) authorized all animal care and experimental procedures (project code: SCXK 2019-0001, date of approval: 14 January 2019; Approval No. SYXK 2014-0003), in compliance with institutional guidelines for the care and use of animals. The FDA of the United States and the European Drug Administration has approved the daily dose of pazopanib as 800 mg. The mice were divided into high-dose and low-dose groups according to the equivalent dose ratio of 88 mg/kg in different groups. The mice were randomly divided into five groups (n=7 per group): the control group, BLM group, nintedanib-treated group (100 mg/kg), low-dose pazopanib-treated group (50 mg/kg), and high-dose pazopanib-treated group (100 mg/kg). Nintedanib was purchased from Macklin

Biochemical (Shanghai, China), and pazopanib was purchased from Dalian Meilun Biotechnology (Dalian, China). For 7–14 days, the mice were given either pazopanib, nintedanib, or water orally. In order to study the fibrotic response, mice were intratracheally injected with BLM (Medicine Co., Tokyo, Japan) at a dose of 2 U/kg body weight. The sham group received the same volume of saline intravenously. The drugs were administered daily the 7th day of modeling and continued through the 14th day. Mice were sacrificed on day 14, and lung tissues were harvested.

### Cell culture

The Mlg and NIH-3T3 cell lines were kindly gifted from Professor Wen Ning of Nankai University. Mlg and NIH-3T3 cells were stimulated with TGF- $\beta$ 1 or pazopanib. Mouse primary pulmonary fibroblasts (PPFs) were isolated from the lung tissues of NaCl- or BLM-treated mice on day 14. All cells were cultured according to the established guidelines. These cells were cultured in Dulbecco's Modified Eagle Medium (DMEM) (Solarbio, Beijing, China) supplemented with 10% fetal bovine serum (Gibco, New York, USA) in an incubator at constant temperature of 37 °C with 5% CO<sub>2</sub>.

### Transfection methods

NIH-3T3 cells were seeded onto glass slides in 24-well plates, after which 1  $\mu$ g of GFP-LC3B or mCherry-GFP-LC3B was transfected into NIH-3T3 cells with polyethylenimine (PEI) (Thermo Fisher Scientific, New York, USA) for 6 hours.

### Western blot

The lysates of cells or tissues were prepared with RIPA buffer (Beyotime, Shanghai, China) supplemented with a cocktail (Sigma, New Jersey, USA) and quantified via a BCA protein assay (Beyotime). Sodium dodecyl sulfate polyacrylamide gel electrophoresis (SDS-PAGE) was used to detect protein expression. After the membranes were incubated with primary and secondary antibodies, immunoreactivity was detected via enhanced chemiluminescence (ECL) (Affinity, New York, USA). The secondary antibodies used were as follows: goat anti-rabbit immunoglobulin G (IgG)-horseradish peroxidase (HRP) (Abcam, London, UK) and goat anti-mouse IgG-HRP (Abcam). The primary antibodies used in this study are listed in *Table 1*.

### *Real-time quantitative polymerase chain reaction (PCR)*

Total RNA was extracted using TRIzol (Thermo Fisher Scientific). The RNA was transcribed using the reverse SYBR Select Master Mix Kit according to the manufacturer's instructions (Tiangen, Beijing, China), followed by fluorescence quantitative real-time PCR (Yeasten, Shanghai, China). We used Celemetor 96 real-time fluorescence quantitative PCR analysis system for real-time fluorescence quantitative PCR detection (instrument batch number: YS80520-2304-00001; Yeasen). PCR primer sequences were as follows:

- ❖  $\beta$ -actin: AGGCCAACCGTGAAAAGATG (forward primer); AGAGCATAGCCCTCGTAGATGG (reverse primer).
- ❖  $\alpha$ -SMA: GCTGGTGATGATGCTCCCA (forward primer); GCCATTCCAACCATCTACTCC (reverse primer).
- ❖ Collagen 1a1: CCAAGAAGACATCCCTGAA GTCA (forward primer); TGCACGTCATCGCAC ACA (reverse primer).
- ❖ Fibronectin (FN): GTGTAGCACAACCT TCCAATTACGAA (forward primer); GGAATTT CCGCCTCGAGTCT (reverse primer).

### *Wound-healing assays*

For the wound healing assay, Mlg and PPF cells were grown on 6-well plates and scraped to form a 100- $\mu$ m wound using sterile pipette tips. Because Mlg cells grow quicker, a scratch test was performed when the density of Mlg cells was 50% and the density of PPF cells was around 100%. The cells were cultured in the presence or absence of pazopanib (2 or 4  $\mu$ M) in serum-free media for 12, 24, 36, or 48 hours. Images at different time points were captured by a light microscope (Nikon, Tokyo, Japan).

### *Luciferase assay*

A luciferase assay was performed by using a luciferase assay system (Promega, Wisconsin, USA) and a Luminoskan Ascent Reader System (Thermo Fisher Scientific).

### *Hematoxylin-eosin staining*

Hematoxylin-eosin staining was applied after the left lung was sectioned into 5  $\mu$ m pieces and embedded in paraffin.

An upright transmission fluorescence microscope was used to gather the stained images, and Image-Pro Plus Version 6.0 (Media Cybernetics, Inc., Rockville, MD, USA) was used for analysis. By analyzing the entire lung tissue area and automatically calculating the total pixel of the area (Pw), the total pixel of the fibrotic area (Pf) was calculated, and the fibrosis ratio was calculated as Pf/Pw.

### *Immunohistochemistry*

After antigen retrieval, the lung tissue sections were incubated with the primary antibody against the detection marker, the color was developed with Digital Audio Broadcasting (DAB), and the nucleus was stained with hematoxylin. ImageJ software (National Institutes of Health, Maryland, USA) was used to analyze the intensity and percentage of stained cells after microscopic imaging.

### *Immunofluorescence*

Mlg cells were plated on glass slides in 24-well plates and then treated with TGF- $\beta$ 1 (5 ng/mL) or pazopanib (2, 4  $\mu$ M) for 24 hours. After fixation with 4% paraformaldehyde in phosphate buffer solution (PBS) for 20 minutes, the cells were washed with PBS and incubated with 0.2% Triton X-100 (Sigma) and 5% bovine serum albumin (BSA) (Sigma) for 30 minutes to block nonspecific binding. The primary antibody was incubated on the cells for an entire night at 4  $^{\circ}$ C, and the secondary antibody (goat anti-mouse IgG conjugated with DyLight 594) was incubated on the cells for one hour at 37  $^{\circ}$ C. Finally, the cells were subjected to nuclear staining with DAPI Staining Solution (Solarbio, Beijing, China). Images were visualized using confocal laser scanning microscopy (Leica SP8, Wetzlar, Germany) and photographed.

### *Hydroxyproline content*

The hydroxyproline concentration in the mouse right lung was determined via the traditional acid hydrolysis method. Briefly, the right lung was immediately dried in an oven and then hydrolyzed at 120  $^{\circ}$ C with 6 N hydrochloric acid for 18 hours. After filtering the residue, 6 N NaOH was used to adjust the pH to 6.5–7.6. The hydroxyproline standard (Sigma) was used to construct a standard curve, and the results were calculated as the  $\mu$ g hydroxyproline/right lung.

### *Lung function measurement*

The lung function of C57BL/6 mice was measured by using an AniRes2005 lung function system (Bestlab, Changsha, China). After anesthesia, the mice were placed in a body drawing box to explore lung function indices, including dynamic compliance (C<sub>dyn</sub>), inspiratory resistance (R<sub>i</sub>), and expiratory resistance (R<sub>e</sub>), forced vital capacity (FVC), forced expiratory volume in 0.1 second (FEV<sub>0.1</sub>), and forced expiratory volume in 0.3 second (FEV<sub>0.3</sub>).

### *Statistical analysis*

The statistical analysis was carried out utilizing GraphPad Prism 9.0. An analysis of significant differences was conducted using a two-tailed Student's *t*-test. The concordance was ascertained using linear regression and Pearson correlation. The means ± standard deviations (SDs) were displayed for the data, and the following are the significance levels: P<0.05, P<0.01 and P<0.001.

## **Results**

### *Pazopanib attenuates BLM-induced pulmonary fibrosis in mice*

We first established a BLM-induced pulmonary fibrosis model and evaluated the therapeutic effect of pazopanib. As expected, pazopanib improved BLM-induced alveolar structure distortion and reduced the collagen concentration and percentage of fibrotic areas (Figure 1A,1B). In addition, compared with those in the model group, the hydroxyproline content in the right lung was lower, and the body weight was greater in the pazopanib-treated group (Figure 1C,1D). The effects of pazopanib treatment on pulmonary function parameters are illustrated in Figure 1E-1J, and the results showed that pazopanib significantly reduced the FVC, FEV<sub>0.1</sub>, FEV<sub>0.3</sub>, R<sub>i</sub>, R<sub>e</sub>, and C<sub>dyn</sub>. Nintedanib, a positive control drug, significantly alleviated pulmonary fibrosis in our study, but its effect was worse than that of pazopanib (Figure 1). In conclusion, pazopanib markedly attenuates BLM-induced pulmonary fibrosis mainly by reducing the percentage of fibrosis and improving pulmonary function.

### *Pazopanib decreased TGF-β1-induced lung fibroblast activation and ECM accumulation in vitro*

TGF-β1 is a key profibrotic factor that promotes the

progression of pulmonary fibrosis disease and is a major promoter of myofibroblast activation, proliferation and differentiation (22,23). Hence, we evaluated the effect of pazopanib on the TGF-β1-induced activation of lung fibroblasts *in vitro*. Western blotting analysis revealed that pazopanib treatment downregulated TGF-β1-induced α-SMA, FN and type 1 collagen (Col 1) expression in a dose-dependent manner, which indicated that pazopanib inhibited fibroblast activation and ECM production (Figure 2A,2B). Immunofluorescence staining for α-SMA also confirmed these findings (Figure 2C). In addition, pazopanib reduced the mRNA expression levels of α-SMA, Col 1 and FN in TGF-β1-activated fibroblasts (Figure 2D-2F). In conclusion, pazopanib inhibited TGF-β1-induced lung fibroblast activation and ECM production *in vitro*.

### *Pazopanib inhibits TGF-β1-induced lung fibroblast migration in vitro*

TGF-β1 can induce the migration of human lung fibroblasts, which is strongly related to the progression of pulmonary fibrosis (24). We tested whether pazopanib had an influence on the migration ability of pulmonary fibroblasts by using a wound healing assay. Pulmonary fibroblasts were incubated with pazopanib and/or TGF-β1 for a series of durations. The control group exhibited a narrow cell wound gap, and the pazopanib treatment group exhibited relative delays in wound closure (Figure 3). Hence, pazopanib significantly suppresses the migration of lung fibroblasts.

### *Pazopanib promotes the apoptosis and autophagy of pulmonary myofibroblasts*

IPF myofibroblasts exhibit apoptosis resistance both *in vivo* and *in vitro* (25). The excessive production of ECM proteins is a major characteristic of IPF, and autophagy controls the turnover of collagen (7). Our previous studies showed that pazopanib treatment can slow the development of pulmonary fibrosis in C57BL/6 mice; therefore, we next explored whether pazopanib had a positive effect on apoptosis and autophagy in lung fibroblasts. Western blotting analysis of pazopanib-treated Mlg cells revealed that the expression levels of cleaved caspase3, cleaved caspase7, and cleaved caspase9 were significantly greater than those in the control group, indicating that pazopanib can promote the apoptosis of lung fibroblasts (Figure 4A).

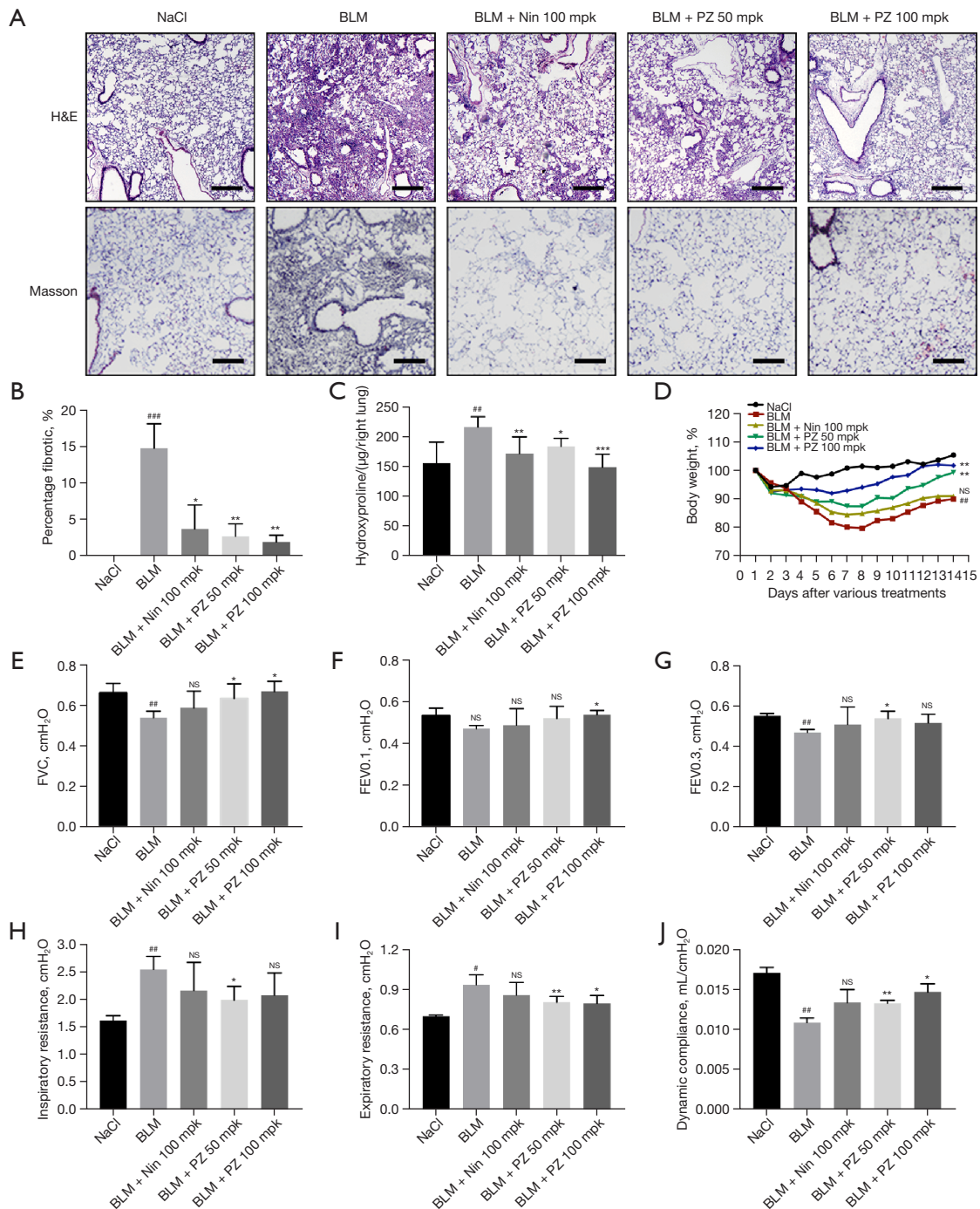


**Figure 1** Pazopanib attenuates BLM-induced pulmonary fibrosis in mice. (A) Photomicrographs of lung sections stained with H&E in each group to observe pulmonary pathologic changes. Scale bars: 50 µm. (B) Fibrotic percent was determined by H&E staining of lung sections. (C) Hydroxyproline content of the right lung in different groups. (D) Average body weight (g) of mice in various groups after the drug treatment. (E-J) Pulmonary function parameters, including FVC, FEV0.1, FEV0.3, inspiratory resistance, expiratory resistance, and dynamic compliance. Data in (B-J) were expressed as mean ± standard deviation. \*, P<0.05; \*\*, P<0.01; \*\*\*, P<0.001 (Student's *t*-test) as compared with BLM-treated group. #, P<0.05; ##, P<0.01; ###, P<0.001 (Student's *t*-test) as compared with NaCl-treated group. H&E, hematoxylin-eosin; BLM, bleomycin; Nin, nintedanib; PZ, pazopanib; mpk, mg/kg; FVC, forced vital capacity; FEV0.1, forced expiratory volume in 0.1 second; FEV0.3, forced expiratory volume in 0.3 second; NS, not significant.

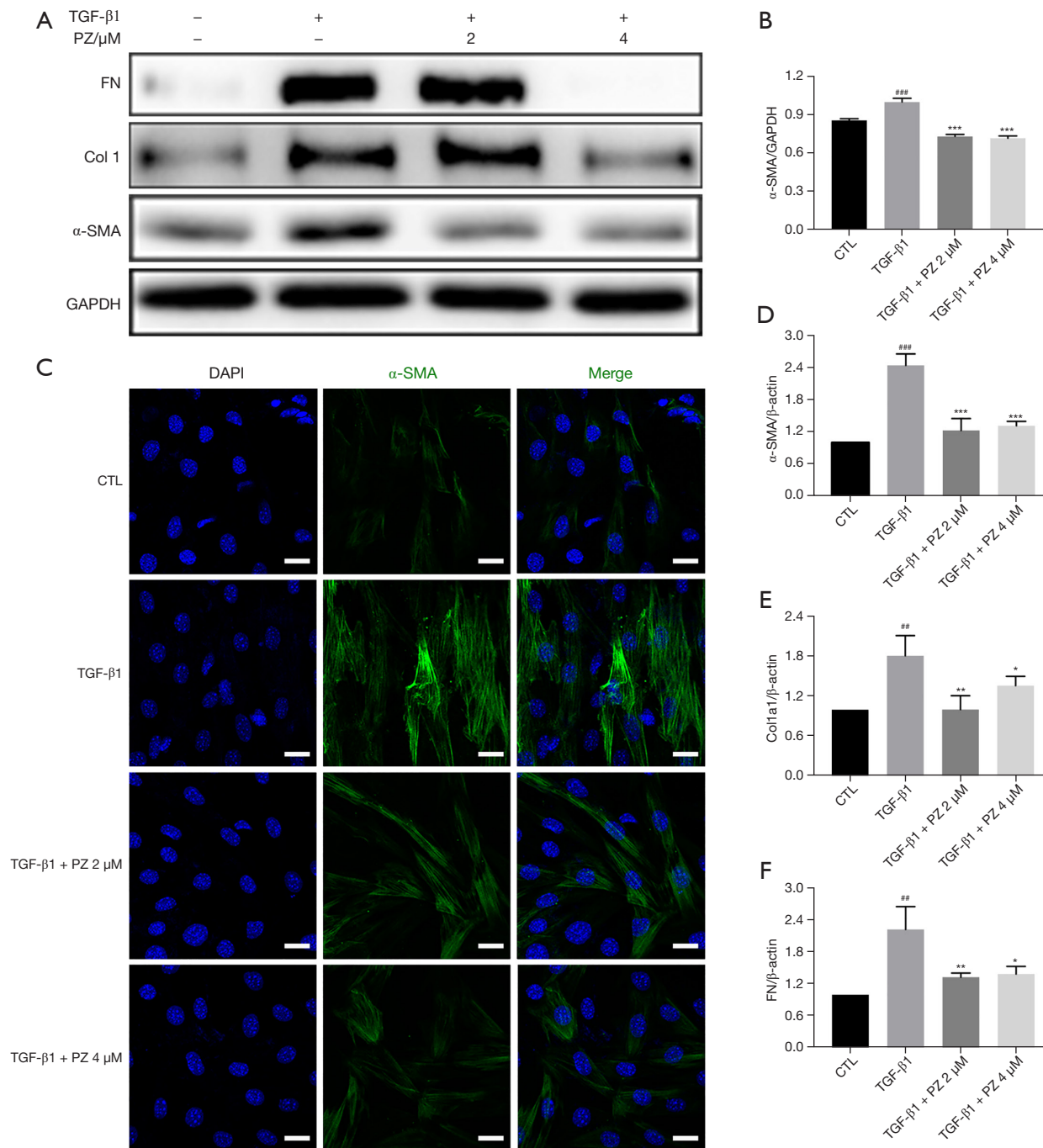


**Figure 2** Pazopanib decreased TGF- $\beta$ 1-induced lung fibroblast activation and ECM accumulation *in vitro*. (A) The Mlg cells were treated with TGF- $\beta$ 1 and/or PZ (2 or 4  $\mu$ M) for 24 hours, and the expression levels of FN, Col 1, and  $\alpha$ -SMA were detected via using Western blot. (B) Densitometric analysis ( $\alpha$ -SMA) of the immunoblot reported in (A). (C) The TGF- $\beta$ 1 and/or PZ (2 or 4  $\mu$ M) were exposed to Mlg cells for 24 hours and analyzed the degree of activation by immunofluorescence technology. Scale bars: 50  $\mu$ m. (D-F) The impact of PZ on TGF- $\beta$ 1-induced increase in the mRNA levels of  $\alpha$ -SMA, Col1a1, and FN in Mlg cells after exposure for 24 hours. GAPDH was used as a loading control. Data in (B,D-F) are mean  $\pm$  standard deviation. <sup>##</sup>,  $P < 0.01$ ; <sup>###</sup>,  $P < 0.001$  (Student's *t*-test) as compared with control group. <sup>\*</sup>,  $P < 0.05$ ; <sup>\*\*</sup>,  $P < 0.01$ ; <sup>\*\*\*</sup>,  $P < 0.001$  (Student's *t*-test) as compared with model group. TGF- $\beta$ 1, transforming growth factor- $\beta$ 1; PZ, pazopanib; FN, fibronectin; Col 1, type 1 collagen; CTL, control; ECM, extracellular matrix.

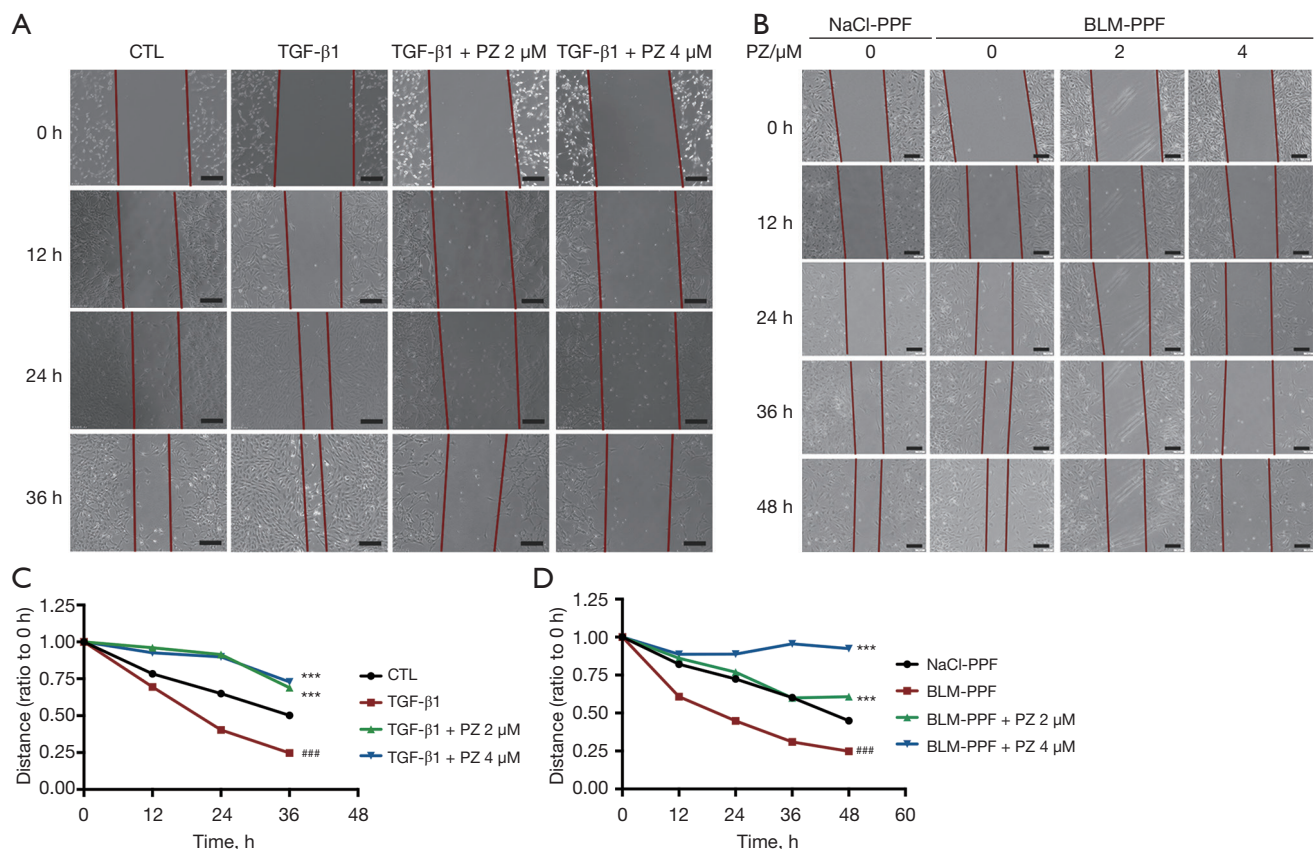


**Figure 3** PZ inhibits pulmonary fibroblast migration in Mlg and PPF cells. (A,C) The Mlg cells were treated with TGF- $\beta$ 1 and/or PZ (2 or 4  $\mu$ M) for 0, 12, 24, and 36 hours. (B,D) The PPF cells isolated from NaCl-treated and BLM-treated mice were incubated with PZ (2 or 4  $\mu$ M) for a series of time points (0, 12, 24, 36, and 48 hours). Scale bars: 100  $\mu$ m. ###,  $P < 0.001$  (Student's  $t$ -test) as compared with control group. \*\*\*,  $P < 0.001$  (Student's  $t$ -test) as compared with model group. CTL, control; TGF- $\beta$ 1, transforming growth factor- $\beta$ 1; PZ, pazopanib; PPF, primary pulmonary fibroblasts; BLM, bleomycin.

The p62 protein is a cargo essential mediator of autophagy. Bafilomycin a1 (Baf a1) and chloroquine (CQ) are autophagy inhibitors. Our results revealed that pazopanib decreased Baf a1- and CQ-induced p62 expression in a dose-dependent manner (Figure 4B,4C). The GFP-LC3B and mCherry-GFP-LC3B plasmids were transfected into NIH-3T3 cells to measure autophagic flux. As expected, pazopanib increased GFP-LC3B puncta formation and the number of Cherry<sup>+</sup> GFP<sup>-</sup> puncta (autolysosomes) (Figure 4D,4E). Hence, pazopanib attenuates BLM-induced pulmonary fibrosis partly by promoting the apoptosis and autophagy of myofibroblasts.

#### *Pazopanib suppresses TGF- $\beta$ 1/Smad and non-Smad signaling*

TGF- $\beta$ 1 plays a vital role in the development of pulmonary fibrosis and can upregulate the phosphorylation of Smad2/3. The stable CAGA-NIH-3T3 cell line was constructed in our previous work, and this luciferase reporter system can assess the activation of TGF- $\beta$ 1/Smad3 signaling (26). TGF- $\beta$ 1 promoted Akt and Erk1/2 phosphorylation compared with that in the control group, consistent with previous reports (27,28). Treatment of CAGA-NIH-3T3 cells with pazopanib (0, 0.5, 1, 2, 4, 8, 16, and 32  $\mu$ M) dose-dependently decreased luciferase activity (Figure 5A).



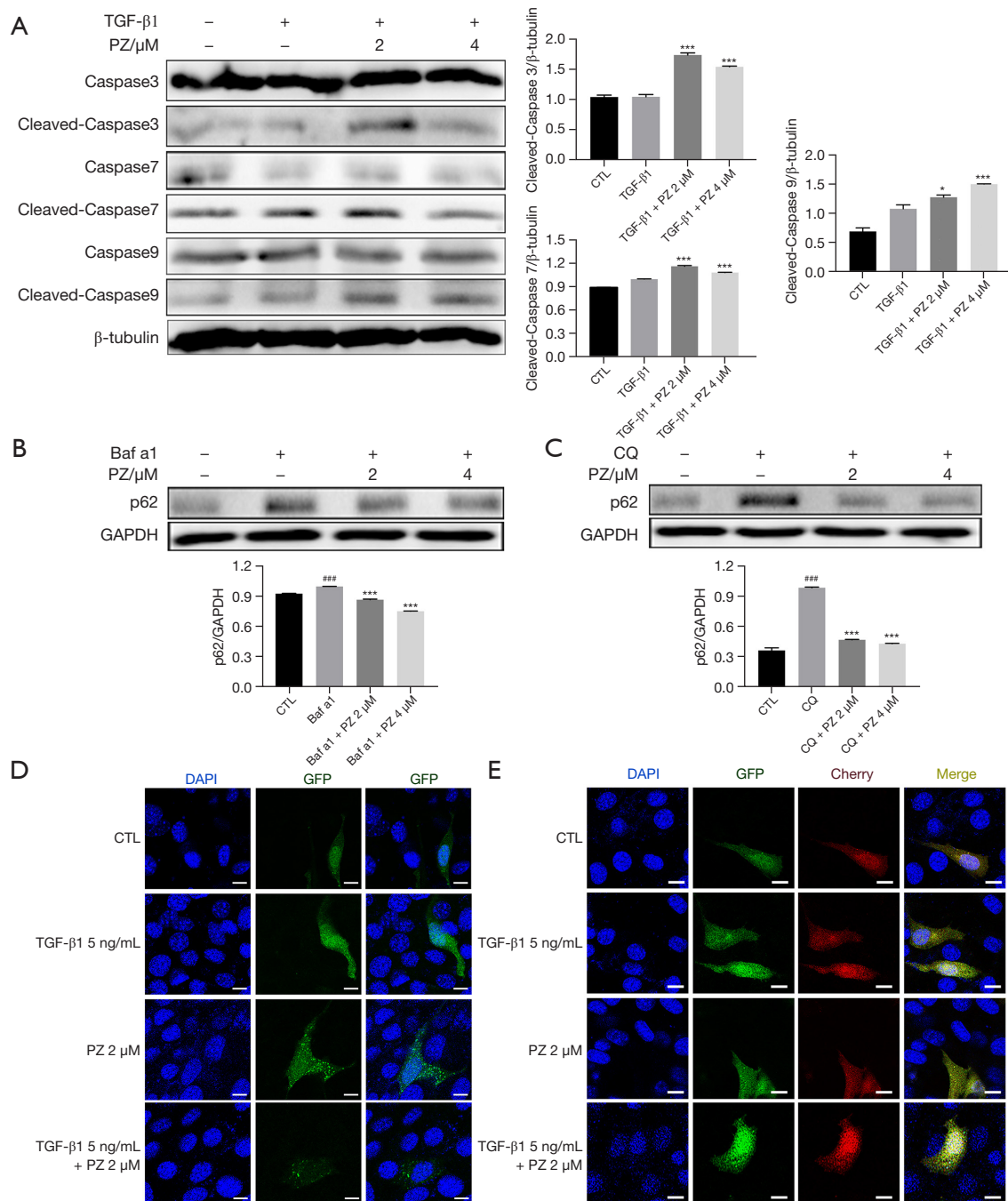


**Figure 4** PZ promotes apoptosis and autophagy of pulmonary myofibroblast. (A) The Mlg cells were incubated with TGF-β1 and/or PZ (2 or 4 μM) for 24 hours. The expression levels of caspase3, cleaved-caspase3, caspase7, cleaved-caspase7, caspase9 and cleaved-caspase9, were detected via using Western blot. The loading control was β-tubulin. (B,C) Mlg cells were exposed to Baf a1/CQ and/or PZ (2 or 4 μM) for 24 hours. The p62 expression level was evaluated by Western blot. GAPDH was used as a loading control. (D,E) The plasmid of GFP-LC3B and GFP-Cherry-LC3B were transfected to NIH-3T3 with PEI, and fluorescence microscopy was used to examine the number of autophagosomes (green puncta) and autolysosome (red puncta) after exposing to TGF-β1 and/or PZ for 12 hours. Scale bars: 50 μm. Data in (A-C) are mean ± standard deviation. <sup>###</sup>, P<0.001 (Student's *t*-test) as compared with control group. \*, P<0.05; <sup>\*\*\*</sup>, P<0.001 (Student's *t*-test) as compared with model group. TGF-β1, transforming growth factor-β1; PZ, pazopanib; CTL, control; Baf a1, bafilomycin a1; CQ, chloroquine; GFP, fluorescent protein; PEI, polyethylenimine.

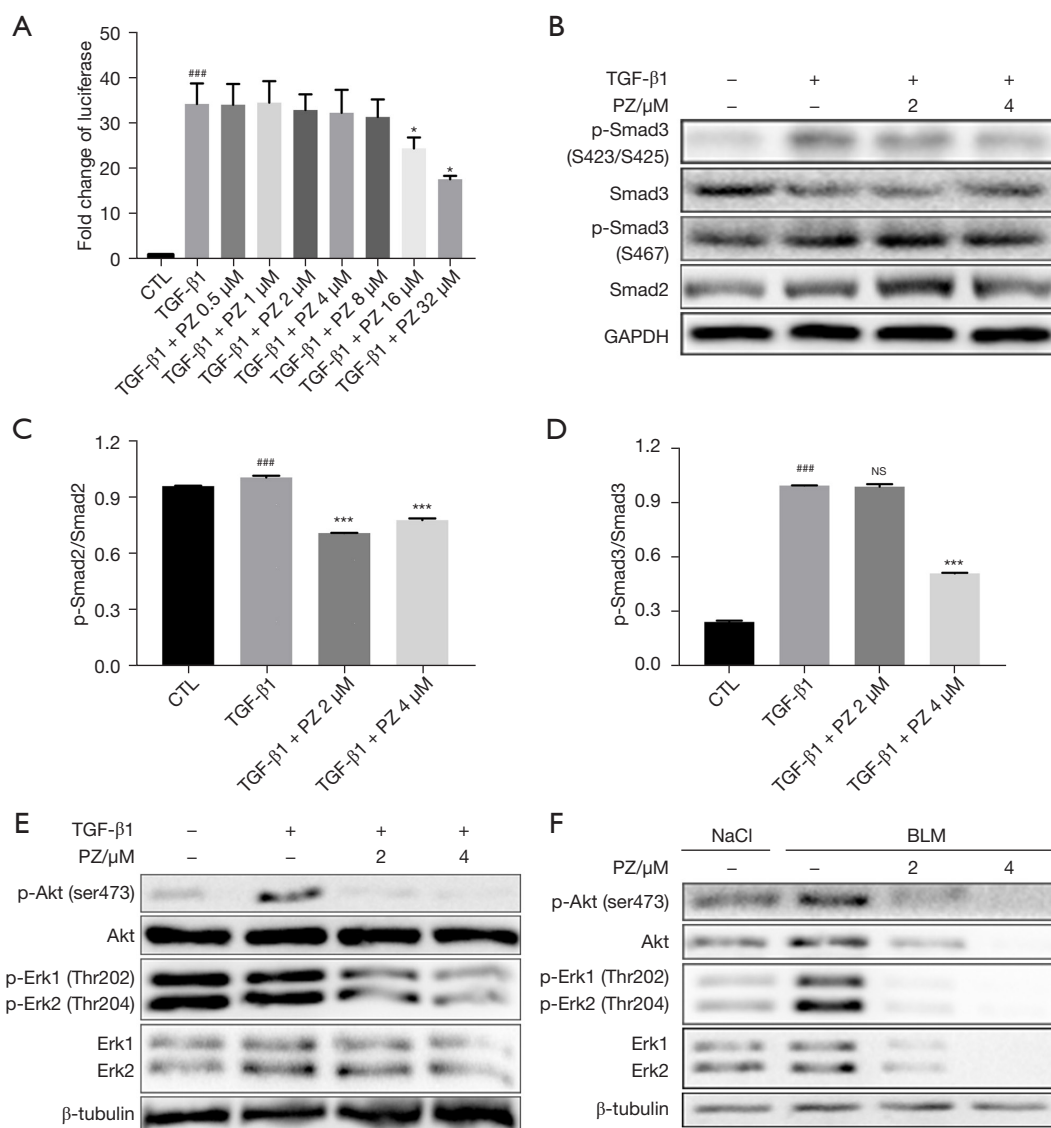


**Figure 5** Pazopanib suppresses TGF-β1/Smad and non-Smad signaling. (A) The CAGA-NIH-3T3 cells were exposed to TGF-β1 and/or a serious concentration (0–32 μM) in serum-free medium for 18 hours. (B) The Mlg cells were treated with/without TGF-β1 and/or PZ (2 or 4 μM) for 30 minutes, and made use of Western bolt to evaluate the p-Smad3 and p-Smad2 expression levels. (C,D) Densitometric analysis of the immunoblot reported in (B). (E) Mlg cells were exposed to TGF-β1 and/or PZ (2 or 4 μM) for 12 hours, then detected for the expression of Akt, Erk and its phosphorylation by Western bolt. (F) The BLM-PPF cells were incubated with PZ (2 or 4 μM) for 24 hours. Data in (C,D) are mean ± standard deviation. <sup>###</sup>, P<0.001 (Student's *t*-test) as compared with control group. <sup>\*</sup>, P<0.05; <sup>\*\*\*</sup>, P<0.001 (Student's *t*-test) as compared with model group. CTL, control; TGF-β1, transforming growth factor-β1; PZ, pazopanib; NS, not significant; BLM, bleomycin; PPF, primary pulmonary fibroblasts.

TGF-β1 (5 ng/mL) strongly phosphorylates Smad3 at Ser423/425, so we used this cellular model to determine whether pazopanib had an impact on the TGF-β1/Smad pathway *in vitro*. As expected, incubating Mlg cells with pazopanib significantly reduced Smad3 and Smad2

phosphorylation (Figure 5B). Mlg cells were incubated with TGF-β1 and/or pazopanib for 12 hours to evaluate whether pazopanib had an impact on TGF-β1/non-Smad (Akt, Erk) signaling. Western blot analysis revealed that pazopanib downregulated the levels of p-Akt (Ser473) and p-Erk1/2

(Thr202/Thr204) (Figure 5C–5E). Next, we verified these results by utilizing PPF cells and found that the results were the same for Mlg cells. In NaCl-PPF and BLM-PPF cells, the levels of Akt and Erk and their phosphorylation were reduced after pazopanib treatment for 24 hours (Figure 5F). These results showed that pazopanib suppresses TGF- $\beta$ 1/Smad and non-Smad signaling *in vitro*.

### ***Pazopanib inhibits fibroblast activation and ECM accumulation and promotes autophagy in vivo***

We further explored whether pazopanib had similar effects *in vivo*. Mice were orally treated with pazopanib (50, 100 mg/kg) on days 7–14 after BLM administration, and the control group was treated with saline. To test the effect of pazopanib treatment *in vivo*, we conducted western blotting to determine the expression and activity levels of important proteins in lung tissues. As shown in Figure 6A, pazopanib significantly decreased the expression of  $\alpha$ -SMA, Col1, FN, p-Smad3 and p62 in lung tissues. The results of immunohistochemical staining also confirmed that pazopanib inhibited the activation of lung fibroblasts, the deposition of collagen, the expression of p62 and the signaling of TGF- $\beta$ 1/Smad3 in a dose-dependent manner (Figure 6B). On the basis of the above studies, pazopanib exerted this effect at a much lower concentration than pirfenidone in lung tissues, demonstrating that it has stronger inhibitory effects on fibroblast activation, ECM production, the expression of p62 and the signaling pathway of TGF- $\beta$ 1/Smad3 (Figure 6). Taken together, these findings suggest that pazopanib attenuates BLM-induced pulmonary fibrosis by suppressing the TGF- $\beta$ 1/Smad3 pathway *in vivo*.

## **Discussion**

ECM accumulation is a fatal characteristic in IPF patients and can lead to irreparable scarring in the lung. It is widely believed that the ECM is secreted mainly by activated fibroblasts and that this accumulation is difficult to reverse entirely in the present study (29). When lung tissues are stimulated continually by chemical materials, fibroblasts can sustain high activation and an uncontrolled state to repair injured lung tissues (1). Obviously, unrepaired scars decrease FVC in IPF patients and eventually lead to death from respiratory failure. Nintedanib is currently the only drug approved for the treatment of IPF. As a tyrosine kinase inhibitor, nintedanib can inhibit a variety of receptor protein tyrosine kinases (PTKs) and non-receptor

PTKs (nPTKs), comprising the receptors for fibroblast growth factor, platelet-derived growth factor, and vascular endothelial growth factor (VEGF). Platelet-derived growth factor receptor (PDGFR), fibroblast growth factor receptor (FGFR) and VEGF receptor (VEGFR) are related to the pathogenesis of IPF. Nintedanib can competitively bind to adenosine triphosphate of these receptors and block intracellular signals related to the proliferation, migration and transformation of fibroblasts related to the pathological mechanism of IPF. Pazopanib is also a small molecule inhibitor of multiple protein tyrosine kinases, including vascular endothelial growth factor receptor and platelet-derived growth factor receptor. It is approved for treating patients suffered from renal cell cancer and advanced soft tissue sarcoma (30). It participates in the inhibition of signal pathway, angiogenesis and cell proliferation.

Our findings showed that pazopanib inhibited myofibroblast activation and ECM production *in vitro*, the same effect was also produced *in vivo* experiments in mice. Pazopanib also promoted mouse lung function in a BLM-induced pulmonary fibrosis model. This finding suggested that the mechanism through which pazopanib improved lung functions was mainly through the inhibition of ECM production. These *in vitro* and *in vivo* results provide an efficient method to support the therapeutic benefits of pazopanib in fibrotic progression.

Many studies have shown that autophagy plays a key role in the pathogenesis of pulmonary fibrosis. The expression level of the autophagy protein p62 in the lung tissue of IPF patients is greater than that in normal individuals (31). When autophagy is inhibited, AICAR (an AMPK activator) is unable to reduce the steady-state levels of collagen induced by TGF- $\beta$ 1 (7). Moreover, the inhibition of autophagic flux induced by profibrotic cytokines can reduce the production of collagen and alleviate pulmonary fibrosis (32). In animal models of BLM-induced pulmonary fibrosis, BLM blocks TFEB-induced autophagic flux by binding to the target ANXA2 (33). In addition, autophagic flux is blocked in alveolar epithelial cells in silica-induced pulmonary fibrosis (34). In summary, autophagy plays an essential role in fibrosis progression because this kind of biological function might promote the degradation of collagen. In our study, pazopanib decreased p62 expression and increased autophagic flux. p62 is a key factor in the regulation of autophagy, mainly through interaction with LC3 (35). However, whether the specific mechanism by which pazopanib reduces p62 expression is by influencing its interaction with LC3 needs to be further investigated.

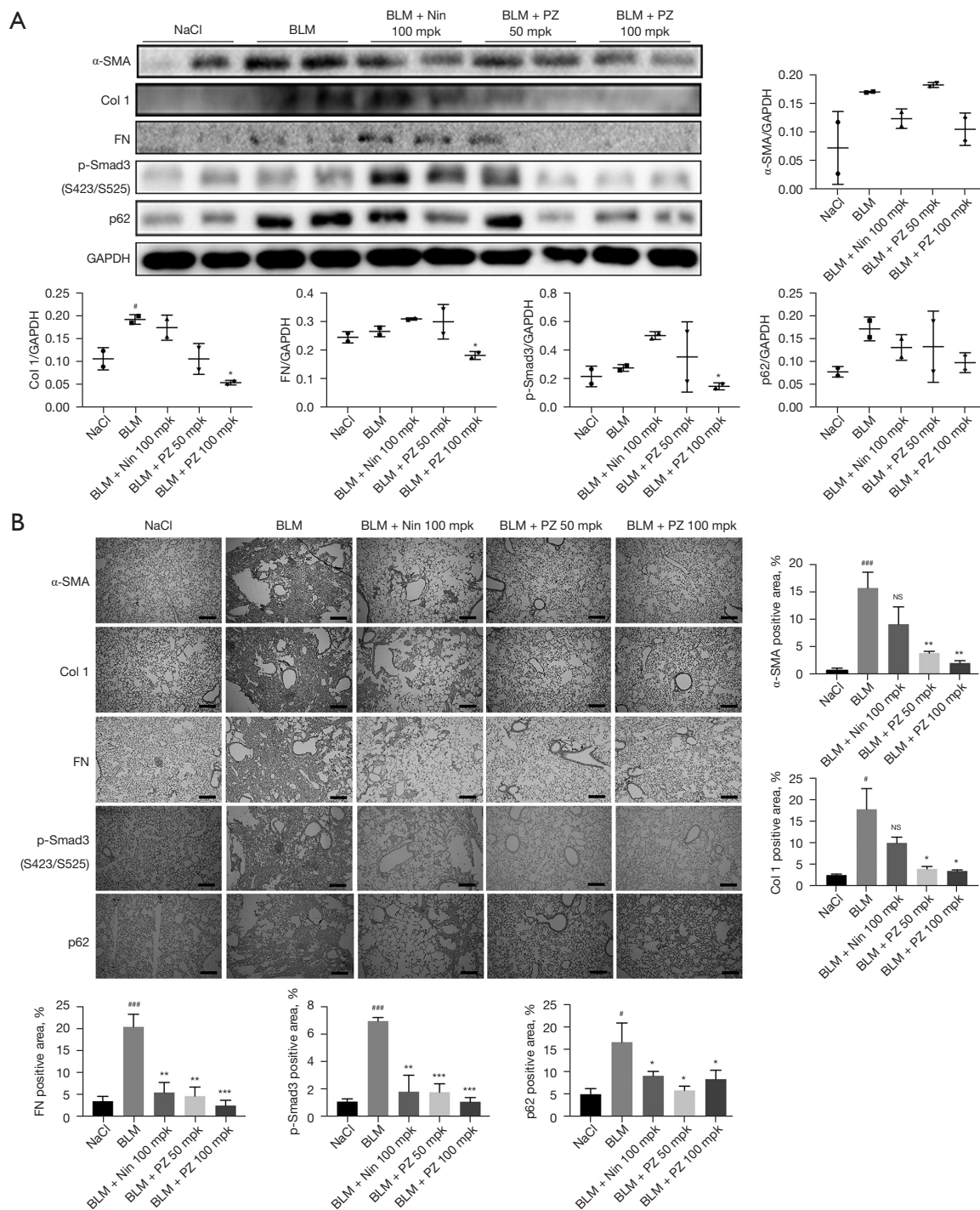


**Figure 6** Pazopanib decreases BLM-induced fibroblast activation, ECM accumulation and promotes autophagy via inhibiting TGF-β1 signaling *in vivo*. (A) The expression levels of α-SMA, Col 1, FN, p-Smad3 and p62 in lung tissues was performed via using Western blot. GAPDH was used as a loading control. (B) Immunohistochemical staining of α-SMA, Col 1 and FN in lung sections (5 μm). Scale bars: 50 μm. Data in (A,B) are mean ± standard deviation. #, P<0.05; ###, P<0.001 (Student's *t*-test) as compared with control group. \*, P<0.05; \*\*, P<0.01; \*\*\*, P<0.001 (Student's *t*-test) as compared with model group. Col 1, type 1 collagen; FN, fibronectin; BLM, bleomycin; Nin, nintedanib; mpk, mg/kg; NS, not significant; TGF-β1, transforming growth factor-β1; ECM, extracellular matrix.

TGF- $\beta$ 1 is a key regulator of the progression of organ fibrosis. Many studies have shown that the binding of TGF- $\beta$  to its receptor activates Smad2 and Smad3 to regulate the expression of ECM genes and pulmonary fibrogenesis (36). In addition, TGF- $\beta$  activates Akt in glomerular mesangial cells by inducing both miR-216a and miR-21 (24). TGF- $\beta$  also activates Erk MAP kinases mainly by activating the TGF- $\beta$  type I receptor to recruit and directly phosphorylate ShcA proteins on tyrosine and serine residues (28). Therefore, the inhibition of the TGF- $\beta$ /Smad and non-Smad (Erk, Akt) signaling pathways efficiently suppresses myofibroblast activation and ECM production to attenuate pulmonary fibrosis. Our results showed that pazopanib inhibited fibroblast activation and ECM deposition mainly by inhibiting the TGF- $\beta$ /Smad and non-Smad signaling pathways *in vitro* and *in vivo*, thus alleviating pulmonary fibrosis.

## Conclusions

In conclusion, our data demonstrated that pazopanib attenuated BLM-induced pulmonary fibrosis in mice. We further explored the pharmacological mechanism of pazopanib, and the results indicated that pazopanib can suppress myofibroblast activation, migration, autophagy, apoptosis and ECM accumulation by downregulating TGF- $\beta$ 1/Smad signaling and the TGF- $\beta$ 1/non-Smad pathway. Pazopanib is a small molecule that is highly active in cancer treatment and might have an equal effect on improving fibrosis progression to benefit IPF patients.

## Acknowledgments

**Funding:** This work was supported by the National Natural Science Foundation of China (Grant No. 82000073), Shenzhen Science and Technology Program (Grant No. JCYJ20210324122006017) and The Foundation of Organ Fibrosis Druggability Joint Research Centre of Nankai and Guokaixingcheng (Grant No. 735-F1040051).

## Footnote

**Reporting Checklist:** The authors have completed the ARRIVE reporting checklist. Available at <https://jtd.amegroups.com/article/view/10.21037/jtd-23-1349/rc>

**Data Sharing Statement:** Available at <https://jtd.amegroups.com/article/view/10.21037/jtd-23-1349/dss>

**Peer Review File:** Available at <https://jtd.amegroups.com/article/view/10.21037/jtd-23-1349/prf>

**Conflicts of Interest:** All authors have completed the ICMJE uniform disclosure form (available at <https://jtd.amegroups.com/article/view/10.21037/jtd-23-1349/coif>). H.R., C.G., Z.W., L.T., S.G., H.Z., and H.Y. are employees of China Resources Biopharmaceutical Co., Ltd. The other authors have no conflicts of interest to declare.

**Ethical Statement:** The authors are accountable for all aspects of the work in ensuring that questions related to the accuracy or integrity of any part of the work are appropriately investigated and resolved. All animal care and experimental procedures were approved by the IACUC of Nankai University (project code: SCXK 2019-0001, date of approval: 14 January 2019; Approval No. SYXK 2014-0003), in compliance with institutional guidelines for the care and use of animals.

**Open Access Statement:** This is an Open Access article distributed in accordance with the Creative Commons Attribution-NonCommercial-NoDerivs 4.0 International License (CC BY-NC-ND 4.0), which permits the non-commercial replication and distribution of the article with the strict proviso that no changes or edits are made and the original work is properly cited (including links to both the formal publication through the relevant DOI and the license). See: <https://creativecommons.org/licenses/by-nc-nd/4.0/>.

## References

1. Wolters PJ, Collard HR, Jones KD. Pathogenesis of idiopathic pulmonary fibrosis. *Annu Rev Pathol* 2014;9:157-79.
2. Mora AL, Rojas M, Pardo A, et al. Emerging therapies for idiopathic pulmonary fibrosis, a progressive age-related disease. *Nat Rev Drug Discov* 2017;16:755-72.
3. Chanda D, Otoupalova E, Smith SR, et al. Developmental pathways in the pathogenesis of lung fibrosis. *Mol Aspects Med* 2019;65:56-69.
4. Huang H. Update in interstitial lung disease 2023. *Zhonghua Jie He He Hu Xi Za Zhi* 2024;47:44-9.
5. Johannson KA, Vittinghoff E, Lee K, et al. Acute exacerbation of idiopathic pulmonary fibrosis associated with air pollution exposure. *Eur Respir J* 2014;43:1124-31.
6. Karimi-Shah BA, Chowdhury BA. Forced vital capacity in idiopathic pulmonary fibrosis--FDA review of pirfenidone

- and nintedanib. *N Engl J Med* 2015;372:1189-91.
7. Rangarajan S, Bone NB, Zmijewska AA, et al. Metformin reverses established lung fibrosis in a bleomycin model. *Nat Med* 2018;24:1121-7.
  8. Ask K, Bonniaud P, Maass K, et al. Progressive pulmonary fibrosis is mediated by TGF-beta isoform 1 but not TGF-beta3. *Int J Biochem Cell Biol* 2008;40:484-95.
  9. Leppäranta O, Sens C, Salmenkivi K, et al. Regulation of TGF-β storage and activation in the human idiopathic pulmonary fibrosis lung. *Cell Tissue Res* 2012;348:491-503.
  10. Wipff PJ, Rifkin DB, Meister JJ, et al. Myofibroblast contraction activates latent TGF-beta1 from the extracellular matrix. *J Cell Biol* 2007;179:1311-23.
  11. Liu H, Sun M, Wu N, et al. TGF-β/Smads signaling pathway, Hippo-YAP/TAZ signaling pathway, and VEGF: Their mechanisms and roles in vascular remodeling related diseases. *Immun Inflamm Dis* 2023;11:e1060.
  12. Schiller M, Javelaud D, Mauviel A. TGF-beta-induced SMAD signaling and gene regulation: consequences for extracellular matrix remodeling and wound healing. *J Dermatol Sci* 2004;35:83-92.
  13. Levine B, Kroemer G. Autophagy in the pathogenesis of disease. *Cell* 2008;132:27-42.
  14. Lock R, Debnath J. Extracellular matrix regulation of autophagy. *Curr Opin Cell Biol* 2008;20:583-8.
  15. Avivar-Valderas A, Bobrovnikova-Marjon E, Alan Diehl J, et al. Regulation of autophagy during ECM detachment is linked to a selective inhibition of mTORC1 by PERK. *Oncogene* 2013;32:4932-40.
  16. Zhang HY, Phan SH. Inhibition of myofibroblast apoptosis by transforming growth factor beta(1). *Am J Respir Cell Mol Biol* 1999;21:658-65.
  17. Pick AM, Nystrom KK. Pazopanib for the treatment of metastatic renal cell carcinoma. *Clin Ther* 2012;34:511-20.
  18. Climent MA, Muñoz-Langa J, Basterretxea-Badiola L, et al. Systematic review and survival meta-analysis of real world evidence on first-line pazopanib for metastatic renal cell carcinoma. *Crit Rev Oncol Hematol* 2018;121:45-50.
  19. Martin-Broto J, Stacchiotti S, Lopez-Pousa A, et al. Pazopanib for treatment of advanced malignant and dedifferentiated solitary fibrous tumour: a multicentre, single-arm, phase 2 trial. *Lancet Oncol* 2019;20:134-44.
  20. Tavallai S, Hamed HA, Grant S, et al. Pazopanib and HDAC inhibitors interact to kill sarcoma cells. *Cancer Biol Ther* 2014;15:578-85.
  21. Olaussen KA, Commo F, Tailler M, et al. Synergistic proapoptotic effects of the two tyrosine kinase inhibitors pazopanib and lapatinib on multiple carcinoma cell lines. *Oncogene* 2009;28:4249-60.
  22. Kennedy WJ, Trejdosiewicz LK, Southgate J. The role of the extracellular matrix, TGF beta and beta 1-integrin in the regulation of normal human urothelial cytodifferentiation. *British Journal of Cancer* 1998;78:45.
  23. Wells RG, Discher DE. Matrix elasticity, cytoskeletal tension, and TGF-beta: the insoluble and soluble meet. *Sci Signal* 2008;1:pe13.
  24. Fang LP, Lin Q, Tang CS, et al. Hydrogen sulfide suppresses migration, proliferation and myofibroblast transdifferentiation of human lung fibroblasts. *Pulm Pharmacol Ther* 2009;22:554-61.
  25. Thannickal VJ, Horowitz JC. Evolving concepts of apoptosis in idiopathic pulmonary fibrosis. *Proc Am Thorac Soc* 2006;3:350-6.
  26. Wang Q, Xiong F, Wu G, et al. SMAD Proteins in TGF-β Signalling Pathway in Cancer: Regulatory Mechanisms and Clinical Applications. *Diagnostics (Basel)* 2023;13:2769.
  27. Kato M, Putta S, Wang M, et al. TGF-beta activates Akt kinase through a microRNA-dependent amplifying circuit targeting PTEN. *Nat Cell Biol* 2009;11:881-9.
  28. Lee MK, Pardoux C, Hall MC, et al. TGF-beta activates Erk MAP kinase signalling through direct phosphorylation of ShcA. *EMBO J* 2007;26:3957-67.
  29. Sun W, Tang H, Gao L, et al. Mechanisms of pulmonary fibrosis induced by core fucosylation in pericytes. *Int J Biochem Cell Biol* 2017;88:44-54.
  30. Miyamoto S, Kakutani S, Sato Y, et al. Drug review: Pazopanib. *Jpn J Clin Oncol* 2018;48:503-13.
  31. Yue YL, Zhang MY, Liu JY, et al. The role of autophagy in idiopathic pulmonary fibrosis: from mechanisms to therapies. *Ther Adv Respir Dis* 2022;16:17534666221140972.
  32. Mi S, Li Z, Yang HZ, et al. Blocking IL-17A promotes the resolution of pulmonary inflammation and fibrosis via TGF-beta1-dependent and -independent mechanisms. *J Immunol* 2011;187:3003-14.
  33. Wang K, Zhang T, Lei Y, et al. Identification of ANXA2 (annexin A2) as a specific bleomycin target to induce pulmonary fibrosis by impeding TFEF-mediated autophagic flux. *Autophagy* 2018;14:269-82.
  34. Zhao X, Wei S, Li Z, et al. Autophagic flux blockage in alveolar epithelial cells is essential in silica nanoparticle-induced pulmonary fibrosis. *Cell Death Dis* 2019;10:127.

35. Katsuragi Y, Ichimura Y, Komatsu M. p62/SQSTM1 functions as a signaling hub and an autophagy adaptor. *FEBS J* 2015;282:4672-8.
36. Hu HH, Chen DQ, Wang YN, et al. New insights into TGF- $\beta$ /Smad signaling in tissue fibrosis. *Chem Biol Interact* 2018;292:76-83.

**Cite this article as:** Huang K, Zhang Q, Ruan H, Guo C, Wu S, Liu Q, Zhang D, Long S, Wang W, Wu Z, Tian L, Gao S, Zhao H, Gu X, Yin H, Yang C. Pazopanib attenuated bleomycin-induced pulmonary fibrosis via suppressing TGF- $\beta$ 1 signaling pathway. *J Thorac Dis* 2024;16(4):2244-2258. doi: 10.21037/jtd-23-1349